

# LMC Microlensing and Very Thick Disks

Geza Gyuk<sup>1</sup> and Evalyn Gates<sup>2,3</sup>

<sup>1</sup>*S.I.S.S.A., via Beirut 2–4, 34014 Trieste, Italy*

<sup>2</sup>*Adler Planetarium, 1300 Lake Shore Drive, Chicago, IL 60605*

<sup>3</sup>*Department of Astronomy & Astrophysics, The University of Chicago, Chicago, IL 60637*

Received \*\*\*

## ABSTRACT

We investigate the implications of a very thick (scale height 1.5 - 3.0 kpc) disk population of MACHOs. Such a population represents a reasonable alternative to standard halo configurations of a lensing population. We find that very thick disk distributions can lower the lens mass estimate derived from the microlensing data toward the LMC, although an average lens mass substantially below  $0.3M_{\odot}$  is unlikely. Constraints from direct searches for such lenses imply very low luminosity objects: thus thick disks do not solve the microlensing lens problem. We discuss further microlensing consequences of very thick disk populations, including an increased probability for parallax events.

**Key words:** Galactic halo: microlensing: dark matter

## 1 INTRODUCTION

Current data from the MACHO collaboration (Alcock et al. 1997) indicate that in the context of a spherical isothermal model with a Maxwellian velocity distribution, some significant fraction of the Galactic halo is composed of MACHOs with masses roughly in the range 0.1 to  $1.0 M_{\odot}$ . Such masses are consistent with several astrophysical candidates for MACHOs – white dwarfs, neutron stars, and black holes – each of which presents serious challenges for stellar formation and evolution theories. However, the MACHO component of the halo, if it is not the major component, as in Cold Dark Matter scenarios, may have a very different distribution from the typically assumed spherical isothermal model. The MACHO distribution may be in a significantly flattened halo and/or, due to dissipation, more centrally condensed. In addition, such a distribution might have a significant rotational component. These possibilities have strong implications not only for the MACHO fraction of the halo, but also for the mass estimates derived from the event durations.

The velocity dispersion and mass density distribution which describe the halo model are crucial input parameters in extracting an estimate of the lens mass from the data. The event duration is given by the radius of the Einstein ring divided by the MACHO velocity transverse to the line of sight, where the Einstein ring radius is a function of the position of the MACHO along the line of sight and the lens mass. The masses of the lenses can only be determined statistically, in the context of an a priori assumption about the distribution and velocity dispersion of the lenses. Such an analysis, using a spherical isothermal model yields a central mass estimate of  $\approx 0.4M_{\odot}$ .

However, as discussed above, the MACHO distribution and velocity dispersion may be very different from that assumed in the standard halo model. Earlier work (Gyuk & Gates 1998) in exploring models with a highly flattened halo and a bulk rotational component has suggested that a very highly condensed model for the MACHO distribution, such as a thick disk, might reduce the MACHO mass estimate from the current data to a level consistent with brown dwarf candidates. Previous explorations (Gates et al. 1998) have indicated that such models may be able to reproduce the observed optical depths toward the Large Magellanic Cloud (LMC) and the Galactic bulge.

The overall shape of the Galactic halo is unknown. Attempts to determine the shape of galactic halo potentials from flaring of the outer Galactic gas layer (Olling 1996; Sackett et al. 1994) point to a flattened halo; flattening of the potential is also supported by simulations of the cold dark matter halo formation (Dubinski J. & Carlberg, R.G. 1991). While it is highly unlikely that the entire halo is in a disk-like configuration, it is not unreasonable to assume that the MACHO component of the halo is significantly more flattened than the dark matter halo. The condensation of a gaseous halo component to form a very thick disk is likely to result in significant star formation and thus the production of a population of lens candidates.

In this paper we explore in detail the consequences of such a lens population. We first define the density and velocity structure, and outline the constraints on these distributions. We then present predictions and observational consequences of such thick disks; in particular we determine the expected frequency of parallax events.

## 2 VERY THICK DISKS

### 2.1 Density

We consider a MACHO population which is distributed in a very thick (fat) disk, whose scale height ranges from 1.5 to 3.0 kpc. The radial profile of these fat disks is assumed to have one of two forms:

$$\begin{aligned}\Sigma(r) &= \Sigma_0 \exp((R_0 - R)/r_d) \\ \Sigma(r) &= \Sigma_0 \frac{R_0 + a}{R + a}.\end{aligned}\quad (1)$$

The first, an exponential disk with scale length  $r_d$ , is similar to the known thick disk population, though as we shall see the surface densities must be much larger. The other, a Mestel disk with core  $a$ , is closer to a very flattened halo.

Such distributions were considered by Gates et al. (1997) in the context of comprehensive Galactic models. The relevant uncertainties in the parameters that describe the various components of the Galaxy and observational constraints on the rotation curve were incorporated in determining viable models. In this paper we focus primarily on the disk component of these models in order to study the implications of such a lens population in detail and only the disk parameters relevant to our conclusions will be discussed.

Since the scale length of the disk is not well known, we consider both 3.0 kpc and 4.0 kpc (Sackett 1997). While the core radius for a possible Mestel disk is completely unconstrained, our conclusions are not strongly dependent on the core radius and therefore we choose  $a = 3.0$  kpc, a value which does not violate any current rotation curve constraints.

Profiles of the known thin and thick disk populations can be fit reasonably well with a theoretically motivated (isothermal)  $\text{sech}^2$  variation in the vertical direction. We thus assume this variation in our models as well. We have, finally, for our model volume densities

$$\begin{aligned}\rho(r, z) &= \frac{\Sigma_0}{2h_z} \exp((R_0 - R)/r_d) \text{sech}^2(z/h_z) \\ \rho(r, z) &= \frac{\Sigma_0}{2h_z} \frac{R_0 + a}{R + a} \text{sech}^2(z/h_z).\end{aligned}\quad (2)$$

We allow both  $\Sigma_0$  and  $h_z$  to vary in our consideration of models.

### 2.2 Velocity Structure

Observations of local stars show that the velocity distribution of a homogenous population of stars in the disk can be adequately represented by an anisotropic gaussian, possibly with a bulk motion with respect to the local standard of rest. We therefore follow many other investigations in taking this as the form for our disk distribution function.

For a flat isothermal disk

$$\sigma_z^2 = 2\pi G\rho_0 h_z^2 = \pi G\Sigma_0 h_z. \quad (3)$$

For the range of  $\Sigma_0$  ( $\sim 100M_\odot/\text{pc}^2$ ) and  $h_z$  ( $\sim 2.0$  kpc) that we will be considering, this results in  $\sigma_z \sim 50$  km/s. If stars in the known thick disk population are considered tracers (with a slightly smaller scale height) for the fat disk, we see that this is consistent with the measured vertical velocity dispersion of 35-60 km/s (Ojha et al. 1996; Casertano, Ratnatunga & Bahcall 1990). We therefore adopt equation 4 for

our calculations of  $\sigma_z$  for the fat disk. In any event, calculations show that small deviations from this relation do not effect our results.

Measurements of the velocity ellipsoid for many varieties of stars, both thick and thin disk, show two fairly constant characteristics (see e.g. (Binney & Tremaine 1987)):

$$\begin{aligned}\sigma_r^2 &\approx 2\sigma_z^2 \\ \sigma_\phi^2 &\approx \sigma_z^2.\end{aligned}$$

Finally, populations with high velocity dispersions have been shown to rotate the galaxy more slowly than those with small dispersions. This asymmetric drift can be roughly quantified (on observational and theoretical grounds, see for example (Binney & Tremaine 1987) or (Ojha et al. 1996)) as

$$v_c - \tilde{v}_\phi = \frac{\sigma_r^2}{120\text{km/s}} \quad (4)$$

where we assume  $v_c = 220$  km/s. Thus we take as our distribution function

$$f = \frac{\rho(r, \phi, z)}{m} \frac{1}{\sqrt{(2\pi)^3 \sigma_r \sigma_\phi \sigma_z}} e^{-\left[\frac{v_r^2}{2\sigma_r^2} + \frac{(v_\phi - \tilde{v}_\phi)^2}{2\sigma_\phi^2} + \frac{v_z^2}{2\sigma_z^2}\right]} \quad (5)$$

where  $\sigma_r$ ,  $\sigma_\phi$ ,  $\sigma_z$ , and  $\tilde{v}_\phi$  vary with position as discussed above.

## 3 CONSTRAINTS

### 3.1 Disk Surface Density

Studies of the distribution of tracer stars perpendicular to the disk put limits on the total (luminous + dark) disk surface density of roughly  $90M_\odot/\text{pc}^2$  (Bahcall, Flynn & Gould 1992). However, such studies can only constrain the column density out to approximately the height of the tracer population (1.0 kpc). We require  $\Sigma_{tot, 1.0} < 90M_\odot/\text{pc}^2$  for our fat disk models. The known thin and thick disk populations, M stars, gas, bright stars, dust etc., give a column density of at most  $\approx 50M_\odot/\text{pc}^2$  (Bahcall 1984; Gould, Flynn & Bahcall 1997), essentially all of which is at a height  $|z| < 1.0$  kpc. We are left then with  $\Sigma_{fat, 1.0} < 40M_\odot/\text{pc}^2$ . For a  $\text{sech}^2$  disk we have

$$\Sigma_0(z) = \Sigma_0 \tanh(z/h_z). \quad (6)$$

The constraint for  $z = 1.0$  kpc is plotted in Figure 1 as a dotted line. For short scale lengths this is a stringent limit. By  $h_z \approx 1$  kpc, however, the constraint on the surface density has loosened considerably and beyond  $h_z = 2$  kpc very little can be said about the surface density and the “disk” has become more like an exponential halo.

### 3.2 Rotation Speed

Measurements of the rotation curve and Oort constants are complicated by our position within the Galaxy. As a very conservative constraint, we adopt the following. We require the rotation speed of the disk at  $R_0$ ,  $v_c(R_0) < 240$  km/s. In the calculation of the circular speed we include known dynamically important components, the bulge and luminous disk, as well as the fat disk. The bulge mass is taken to

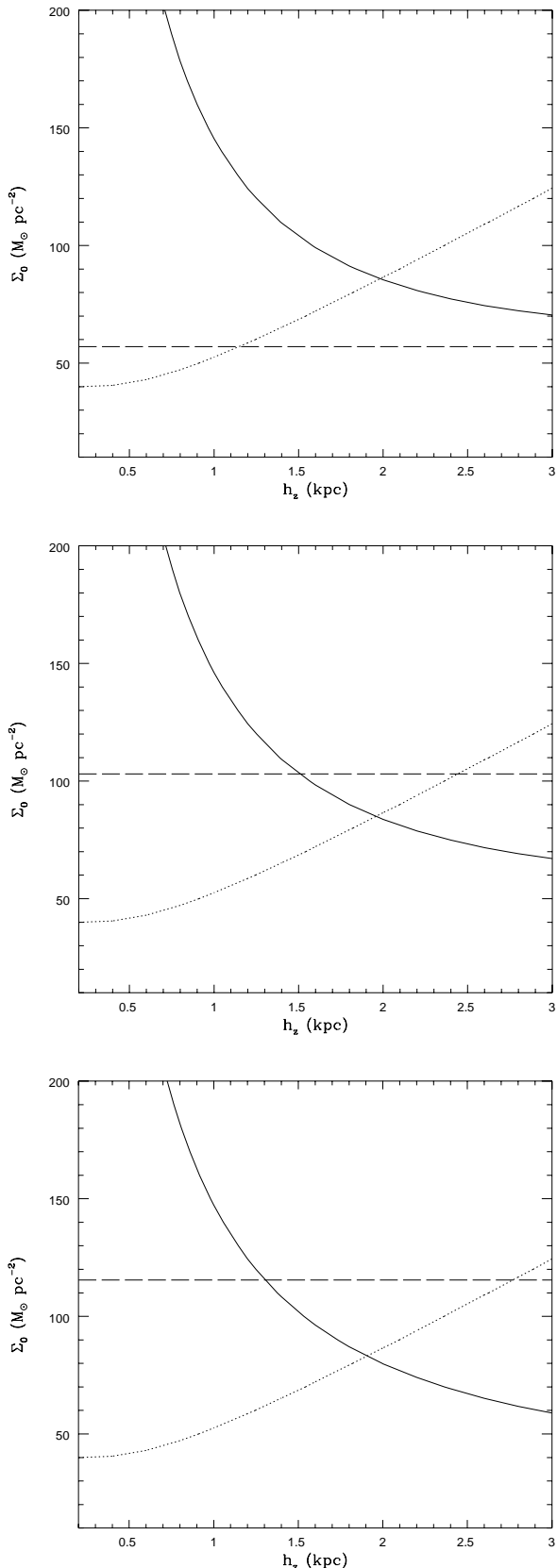


**Figure 1.** Constraints on very thick disks: The region above the dotted line is excluded due to the local surface density constraint ( $\Sigma_{tot,1.0} < 90M_{\odot}/pc^2$ ); above the dashed line is excluded due to rotation curve constraints; and below the solid line the LMC optical depth is less than  $1.0 \times 10^{-7}$  for (a) the 3.0 kpc exponential disk, (b) the 4.0 kpc exponential disk, (c) the Mestel disk.

be  $2 \times 10^{10} M_{\odot}$ . We assume an exponential radial profile for the luminous thin disk with, as discussed above,  $\Sigma_0 = 50 M_{\odot}/pc^2$  and  $r_d = 3.0$  or  $4.0$  kpc depending on the model.

In the thin disk approximation the rotation curve for an exponential disk is

$$v_E^2(R) = 4\pi G \Sigma_0 e^{R_0/r_d} r_d y^2 [I_0(y)K_0(y) - I_1(y)K_1(y)] \quad (7)$$

where  $y = R/2r_d$ . For the Mestel disk in the coreless approximation ( $a = 0$ ) we have very simply

$$v_M^2(R) = 2\pi G \Sigma_0 R_0, \quad (8)$$

which gives a flat rotation curve. We calculate the bulge component of the rotation curve as for a Kepler point source. Thus we ask that

$$v_{lumdisk}^2(R_0) + v_{bulge}^2(R_0) + v_{MACHOs}^2(R_0) < (240 \text{ km/s})^2 \quad (9)$$

where we have left out the halo component to be as generous as possible. The luminous disk and the bulge together contribute about 160–180 km/s leaving only  $\approx 180$  km/s maximum for the MACHOs. This translates into  $\Sigma_0 < 60, 105, 115 M_{\odot}/pc^2$  for the exponential disk with scale lengths 3 kpc, and 4 kpc, and the Mestel disk respectively. These limits are plotted as horizontal dashed lines in Figure 1, independent of  $h_z$ . Note that for high  $h_z$  this limit is much stronger than the column density limits.

### 3.3 Optical Depth

The optical depth to microlensing is given by

$$\tau = \frac{4\pi G}{c^2 D_s} \int_0^{D_s} x(D_s - x)\rho(x)dx \quad (10)$$

where  $D_s$  is the distance to the source and  $x$  is the observer-lens distance. The MACHO collaboration has reported an optical depth toward the LMC of  $2.1_{-0.7}^{+1.1} \times 10^{-7}$  ( $2.9_{-0.9}^{+1.4} \times 10^{-7}$ ) corresponding to 6 (8) microlensing events in their 2 year data (Alcock et al. 1997). We consider a lower limit to the optical depth predicted by our models of  $1.0 \times 10^{-7}$ , approximately one and a half sigma below the MACHO 6-event data. This limit is plotted as a solid line in Figure 1. Because most of the lensing in this class of models takes place close to the observer where the microlensing tube is narrow, high surface densities are required. Further, as the scale height is decreased, the lensing moves closer to the observer where the Einstein radius is smaller and thus it is very difficult to produce enough lensing even with extremely high surface densities.

The first 3 constraints are shown in Figure 1. A few points are immediately obvious. First, the limit on the column density within  $\pm 1.0$  kpc is independent of the disk model since it is purely a local measure. Second, the optical depth is only weakly dependent on the precise model for the disk with the dependence becoming stronger as the scale height increases. This again reflects the local nature of the microlensing: since the fall off above the plane of the disk is exponential for small scale heights most of the microlensing occurs close to the observer where the radial dependence of the density is relatively unimportant. As the scale height increases however, the microlensing increasingly samples regions distant from the observer where the radial coordinate is substantially different. The most important difference between models is the upper limit on the surface density from

the rotation constraints, which varies from  $60M_{\odot}pc^{-2}$  for the 3.0kpc exponential disk to  $115M_{\odot}pc^{-2}$  for the Mestel disk. Short scale length exponentials have much more mass within the solar circle for a given value of  $\Sigma_0$ .

As expected, models with scale heights smaller than 1 kpc are thoroughly ruled out. Thin or thick disks cannot provide sufficient microlensing optical depth toward the LMC. Microlensing is so inefficient for these small scale heights that column density constraints are as much as an order of magnitude lower than needed for  $\tau_{\text{LMC}}$ . As the scale height increases, however, microlensing becomes more efficient and the required surface density decreases to meet the column density constraints at about  $h_z = 2.0\text{kpc}$ ,  $\Sigma_0 = 80M_{\odot}pc^{-2}$  in all models. This is where the rotation constraints figure most strongly. For the more highly condensed model ( $r_d = 3.0\text{kpc}$ ), the density increases rapidly towards the center resulting in a higher rotation velocity for a given surface density. Thus taken together, the three constraints eliminate the short scale length models entirely and restrict the distributed models (long scale length exponential and mestel) to a small allowed region with scale heights  $h_z \approx 2 - 3\text{kpc}$  and surface densities,  $\Sigma_0 \approx 70 - 100M_{\odot}pc^{-2}$ .

### 3.4 HST and Luminosity Constraints

In these fat disk models microlensing takes place closer to the observer than in the standard halo models and thus where the microlensing tube is narrower. To obtain the same optical depth the density locally must therefore be greater. It is thus of interest to examine if searches for faint white dwarfs in the Hubble Deep Field can place significant limits on such models. Flynn et al. (1996) examined the HDF for objects fainter than  $m_I = 24.63$  and redder than  $V - I = 1.8$  down to a limiting magnitude of  $m_I = 26.3$ . They found no such objects in the  $\Omega = 3.72 \times 10^{-7}$  steradian field of the HDF. For an object of I-band absolute magnitude  $M_I$  the volume probed is thus

$$V = 0.9 \frac{\Omega}{3} 10^{[3+0.6(m_I - M_I)]} pc^3. \quad (11)$$

Even for relatively bright objects the maximum distance probed is not very large. Assuming a constant density the number of MACHOs expected in this volume is then

$$N = 0.9 \frac{\rho_0}{m} \frac{\Omega}{3} 10^{[3+0.6(m_I - M_I)]} \leq 3 \quad (12)$$

where the  $\leq 3$  is to be consistent with the non-detection of such objects. For  $\rho_0 = \Sigma_0/2h_z$  this yields

$$M_I > \frac{5}{3} \log_{10} \left[ \frac{\Sigma_0}{2h_z m} \right] + 18.92. \quad (13)$$

with  $\Sigma_0$  in  $M_{\odot}pc^{-3}$ ,  $m$  in  $M_{\odot}$  and  $h_z$  in pc.

For a given mass we can then calculate the minimum magnitude for MACHOs to avoid detection in the HDF as a function of both  $\Sigma_0$  and  $h_z$ . However, for any single mass, this procedure will not be consistent for all combinations of  $\Sigma_0$  and  $h_z$  since this mass may be unlikely or even ruled out for those values. Instead for each combination we use the mass estimated from the microlensing event durations (see next section for these calculations). A contour plot of the minimum magnitudes thus obtained is shown in Figure 6. Magnitudes for the allowed region are  $M_I \approx 16 - 17$ . Comparison of the local volume density for a typical fat disk

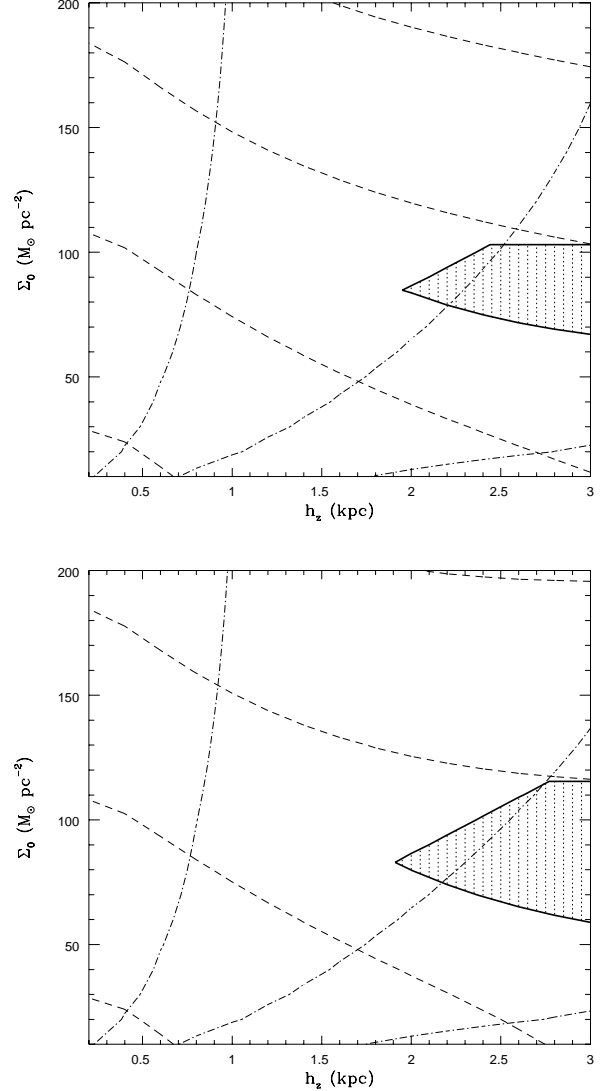


**Figure 2.** Mass and luminosity constraint contours: Contours are  $l=16,17$  and  $18$  from the right and  $m=0.1, 0.2, 0.3$  and  $0.4 M_{\odot}$  from the bottom. The shaded region corresponds to the range of  $\Sigma_0$  and  $h_z$  not excluded by the constraints shown in Figure 1. (a) the 4.0kpc exponential disk. (b) the Mestel disk

model,  $0.02M_{\odot}pc^{-3}$ , to the volume density/age relationship presented by (Graff et al. 1997) shows that the MACHOs must be at least 13 Gyr old and more likely in the 15-17 Gyr range. The fat disk must have formed in the very earliest stages of the formation of the Galaxy.

## 4 PREDICTIONS AND OBSERVATIONAL CONSEQUENCES

### 4.1 Microlensing Rate and MACHO masses

The assumption of the velocity structure of the fat disks we are considering allows us to calculate not only the optical depth, but also the microlensing rate to the LMC. In combination with the optical depth we can find the expected average duration for events for a given model,

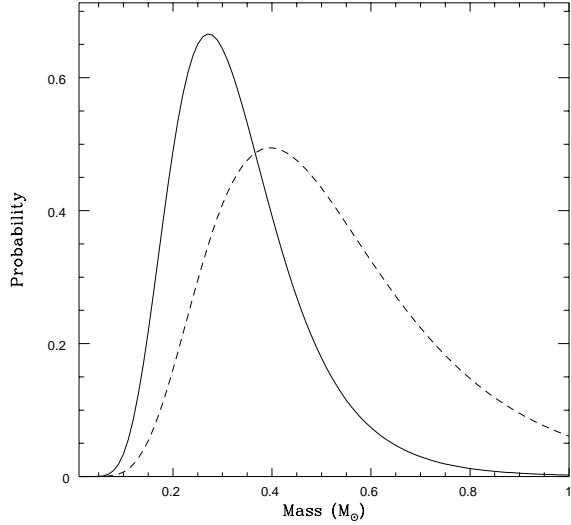


**Figure 3.** Probability vs MACHO mass for Mestel disk (solid line) and standard halo (dashed line).

$$\bar{t}_{model} = \frac{\tau}{\Gamma}. \quad (14)$$

However, unlike the optical depth, the rate depends on the mass of the MACHOs,

$$\Gamma = \Gamma_{1M_{\odot}} \sqrt{\frac{1M_{\odot}}{m}} \quad (15)$$

and hence this average duration is also a function of mass. Comparing the calculated durations to the average observed duration,  $\approx 60$  days we find,

$$\frac{M_{est}}{1M_{\odot}} = \left[ \bar{t}_{obs} \frac{\Gamma_{1M_{\odot}}}{\tau_{model}} \right]^2. \quad (16)$$

where the rate is calculated for  $1M_{\odot}$  MACHOs. Contours of this mass estimate for the range of  $\Sigma_0$  and  $h_z$  are shown in Figure 2. We see that the estimated MACHO mass is  $\sim 0.3M_{\odot}$  for the entire allowed region regardless of the type of disk. Fat disks are not a panacea for the MACHO mass estimate problem. We calculate the distribution of Einstein crossing times for our models as a function of MACHO mass and from this we can calculate the probability for a given MACHO mass to produce the observed distribution of event crossing times. We show in Figure 3 the probability as a function of mass for a Mestel disk with  $\Sigma = 90M_{\odot}\text{pc}^{-2}$ ,  $h_z = 2.5\text{kpc}$ . Brown dwarf masses, while not ruled out at the two sigma level, are unlikely. It is generically true for all of the models we examine that brown dwarf masses are no more likely for than for the standard halo models. This is so because although the average predicted mass is smaller, the dispersion is also slightly smaller and thus the probability for low masses is about the same.

#### 4.2 Total Mass in MACHOs

The analysis of the LMC microlensing events in the context of extended halos yields a robust estimate of the total mass in MACHOs within 50 kpc of  $M_{\text{baryons}} \approx 2 \times 10^{11}M_{\odot}$  in order to produce an LMC optical depth of about  $2 \times 10^{-7}$ .

The production of  $2 \times 10^{11}M_{\odot}$  in white dwarfs requires a much greater metal abundance than is seen unless somewhat ad-hoc efficient galactic winds are invoked to blow the metals out into the intergalactic medium. As discussed in Gates et al. 1998, MACHOs in a very thick disk configuration can reduce this mass estimate, but only slightly. The total mass in a typical very thick disk is  $6.7 \times 10^{10}M_{\odot}$ , which results in an optical depth of about  $1.3 \times 10^{-7}$ . This is approximately 1/2 of the mass that would be required for a halo distribution of MACHOs which would produce the same optical depth. Basically, this reduction can be understood because most microlensing is due to lenses within about 20kpc of the Sun for either configuration. The very thick disk has less mass beyond that distance than a halo. In addition, we note that since the halo of the Galaxy extends far beyond the LMC, a standard halo distribution of MACHOs must be abruptly cut off at 50kpc in order to avoid a much larger total mass in MACHOs which would be even more difficult to reconcile with a white dwarf scenario.

#### 4.3 $\tau_{SMC}/\tau_{LMC}$

Strong flattening of the microlensing population also leaves its mark on the variation of optical depth as a function of direction (Sackett, P. & Gould, A. 1993; Frieman & Scocimarro 1994). In Figure 4 we show  $\alpha = \tau_{SMC}/\tau_{LMC}$  as a function of  $h_z$ . For very flat disks ( $h_z \approx 0.3\text{kpc}$ )  $\alpha$  is the same for both models. All the lensing is local, the global configuration of the MACHOs is irrelevant, and the limiting formula for lensing through a thin disk can be applied. This predicts a value  $\tau_{SMC}/\tau_{LMC} = \sin^2(b_{LMC})/\sin^2(b_{SMC}) = 0.60$ . As  $h_z$  increases however, the configuration becomes less flat and lensing occurs further from the observer. Since the line of sight towards the SMC probes closer to the galactic center, with increasing scale height the SMC direction passes through denser material than the LMC line of sight and so  $\alpha$  increases to about 1.0 by  $h_z = 3.0\text{kpc}$  for the exponential disk model. For the Mestel disk the density increases less strongly with decreasing radius and so this effect is not as large, with  $\alpha$  reaching only 0.75 for  $h_z = 3.0\text{kpc}$ . By comparison, for a standard spherical halo  $\alpha \approx 1.5$ ; for a flattened (E6) halo  $\alpha \approx 1.0$ .

The MACHO and EROS collaborations have recently announced the first detection of a microlensing event towards the SMC. While it is not possible to draw conclusions from a single event, an estimate of the ratio of  $\tau_{SMC}/\tau_{LMC}$  may be determined within the next 5 years or so.

#### 4.4 Duration and Distance Distribution of Events

The distribution of event durations for a typical fat disk model is shown in Figure 5 as a solid line. For comparison, the distribution for a standard isothermal halo is also shown as a dashed line. It is clear that distinguishing between these models on the basis of event durations will require many events. The distribution of events with distance given in Figure 6 shows more clearly the differences between the two models. Very thick disk models concentrate the lensing much closer to the observer with a typical distance of perhaps 5 kpc. In the standard halo case the typical distance is closer to 15 kpc. Although (as discussed in the next section) the

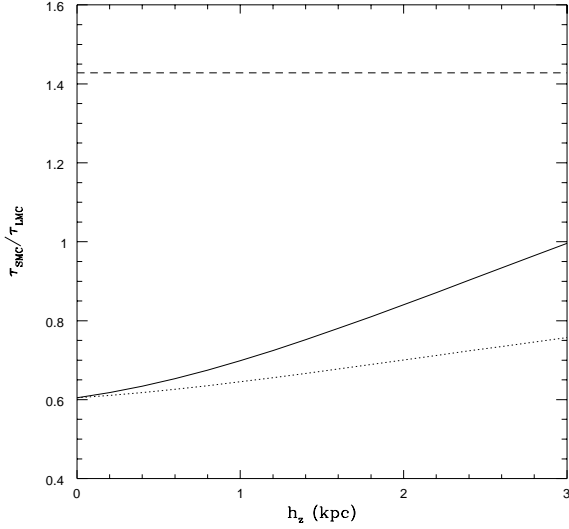


**Figure 4.**  $\tau_{\text{SMC}}/\tau_{\text{LMC}}$  for 4.0kpc exponential disk (dotted line), Mestel disk (solid line) and standard halo (dashed line).

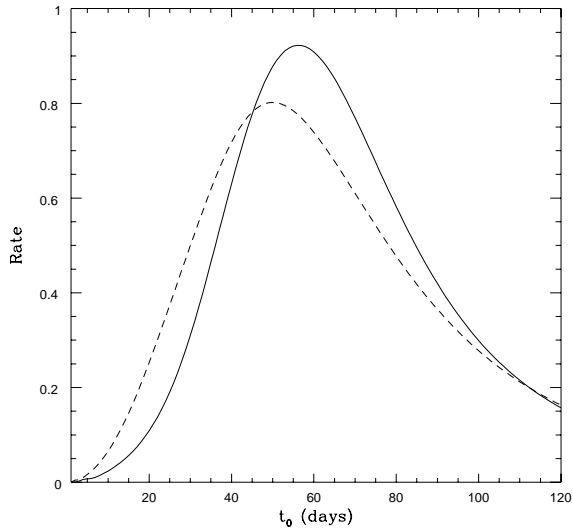


**Figure 5.** Distribution of event durations for a typical thick disk model ( $r_d = 4.0\text{kpc}$ ,  $h_z = 2.5\text{kpc}$ ,  $\Sigma_0 = 90M_\odot/\text{pc}^2$ ) (solid line) and standard halo (dashed line).

fractional rate of parallax events is small, it is possible that the two models could be distinguished with relatively fewer events based on the distances derived.

#### 4.5 Parallax Events

The canonical microlensing light curve is based on a number of assumptions, among which is a constant transverse velocity. Since microlensing events have a non-zero duration, the motion of the Earth in its orbit around the Sun breaks this idealization. For most microlensing events the resulting modification of the light curve is small. For longer events, however, the effect of the Earth's motion is more apparent. The detection of such a modification to the standard

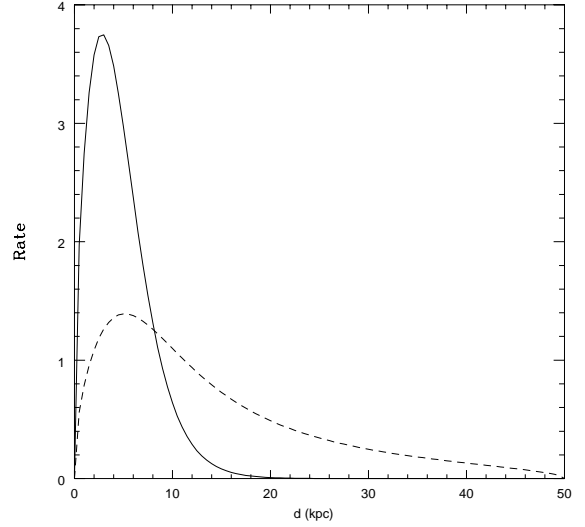


**Figure 6.** Distribution of observer-lens distance for a typical thick disk model  $r_d = 4.0\text{kpc}$ ,  $h_z = 2.5\text{kpc}$ ,  $\Sigma_0 = 90M_\odot/\text{pc}^2$ ) (solid line) and standard halo (dashed line).

light curve is interesting because it allows one to partially break the degeneracy between lens distance, mass and velocity (Gould 1992).

We follow Gould (1998) and define the quantity

$$\gamma = \frac{v_\oplus}{\tilde{v}} \frac{2\pi t_e}{\text{yr}} \cos \phi, \quad (17)$$

which measures the ratio of the earth's acceleration along  $\tilde{v}$  (the projected lens velocity vector) during the event and  $|\tilde{v}|$  itself. This gives us an approximate measure of the strength of the parallax effect of an event. For a given event duration the effect increases as the observer-lens distance and the typical lens velocity decrease. Thus, a typical halo ( $\langle v \rangle \approx 200\text{km/s}$ ,  $\langle x \rangle = 1/4$ ) event will have  $\gamma \approx 0.05$  whereas if the MACHOs are arranged in a thick disk configuration ( $\langle v \rangle \approx 100\text{km/s}$ ,  $\langle x \rangle = 1/10$ ) then typically  $\gamma \approx 0.11$ . We thus expect an increase in the number of observed parallax events for lenses in a fat disk configuration.

In order to more carefully estimate the increase in expected parallax events, we have performed a Monte Carlo analysis of lensing events for lenses in a fat disk and a halo distribution. We sample the light curve for each event in a manner chosen to correspond roughly to the present surveys: daily measurements, 10% photometry, and 5 year baseline, in order to generate the data. We also consider an experiment with 1% photometry for comparison. We then fit a first order parallax light-curve to the data and determine Gould's  $\gamma$  parameter (Gould 1998) as a measure of the strength of the parallax effects.

The distribution of measured  $\gamma$ 's can then be used to distinguish between very thick disk and halo lens distributions. In Figure 7 we present the cumulative probability distributions for  $\gamma$  for a thick disk and a halo. The ability of an experiment to distinguish between these lens distributions will depend on the number of events and photometry. We find that an experiment with 1% photometry and 15 events can distinguish between a very thick disk and a halo with a significance of about 5%, while an experiment with 10%

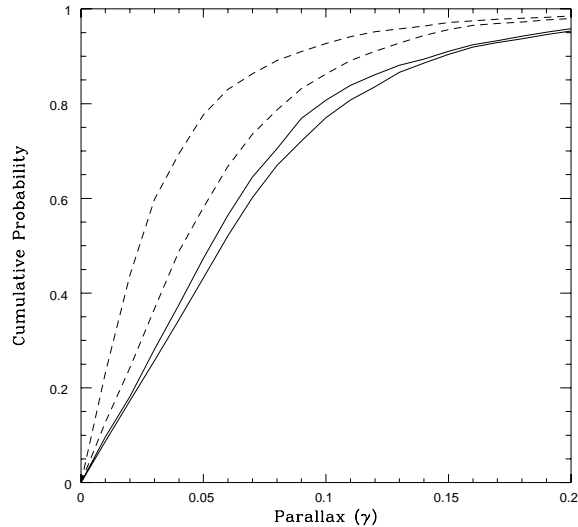


**Figure 7.** Cumulative distribution of the  $\gamma$  parallax parameter for the halo (dashed lines) and thick disk (solid lines) scenarios. Curves for both 1% photometry (left) and 10% photometry (right) are shown. Neither blending nor backgrounds such as binary sources/lenses have been taken into account.

photometry is unable to do so. With 10% photometry at least 75 events are required. We note that these estimates do not include backgrounds from binary source and lens events, whose light curves can mimic parallax effects. However, future observations are likely to include more finely sampled light curves from followup data on alerted events. Such detailed light curves will increase the ability to discriminate between parallax and binary lens or source effects in at least some of the cases.

## 5 CONCLUSIONS

Microlensing studies have yielded much exciting data in the past few years and are continuing to survey different lines of sight through the Galaxy in order to probe the Galactic halo. However, the conclusions that can be drawn from the data to date are very model dependent – assumptions about the distribution of the lenses and their velocity structure have a strong impact on their interpretation. Thus we need to examine a wide range of reasonable lens distributions.

Very thick disks present a reasonable alternative to a halo population of lenses. If the lenses are stellar remnants, it seems likely that their configuration will be more condensed than that of a standard non-baryonic halo. While we have found that very thick disks cannot lower the lens mass estimate to the brown dwarf regime, they have the advantage that their total mass in MACHOs is somewhat less than that for a standard halo that is truncated at 50kpc (and much less than a MACHO halo which traces the extended dark halo out to at least 100kpc.) A thick disk distribution cannot produce an optical depth toward the LMC of more than about  $1.5 \times 10^{-7}$ . However, it can explain (within the experimental uncertainties) all or a significant fraction of the current optical depth estimates.

As more events are detected, it may be possible to dis-

tinguish between very thick disk and halo lens distributions. The most promising avenue for such a discriminant is the observation of parallax events. Because disk lenses would be both closer and on average slower than halo lenses we expect a higher rate of such events for a disk population. Although the survey experiment light curve measurements can only marginally discriminate between disk and halo distributions for reasonable numbers of events, a modest expenditure of telescope time to obtain one percent photometry on all the Magellanic cloud events should be capable of making the distinction very clearly.

## REFERENCES

- Alcock C. et al. 1997, *ApJ*, 486, 697  
Bahcall J. N. 1984, *ApJ* 276, 169  
Bahcall J., Flynn C., & Gould A. 1992, *ApJ* 389, 234  
Binney J. & Tremaine S. 1987, *Galactic Dynamics* (Princeton University Press)  
Casertano S., Ratnatunga K., & Bahcall J. 1990, *ApJ*, 357, 435  
Dubinski J. & Carlberg, R.G. 1991, *ApJ*, 378, 496  
Flynn, C., Gould, A. & Bahcall, J.N. 1996, *ApJ*, 466, L55  
Frieman, J. & Scoccimarro, R. 1994, *ApJL*, 431, L23  
Gates, E., Gyuk, G., Holder, G. & Turner, M.S. 1998, to appear in *MNRAS*  
Gould, A., 1992, *ApJ*, 392, 442  
Gould A., Flynn C., & Bahcall J.N., 1997, *ApJ*, 482, 913  
Gould, A., 1998, submitted to *ApJ*, astro-ph/9802132  
Graff, D., Laughlin, G., & Freese, K. 1997, *astro-ph/9704125*  
Gyuk G., & Gates E. 1998, *MNRAS* 294, 682  
Ojha D., Bienayme O., Robin A., Creze M., & Mohan V. 1996, *A&A*, 311, 456  
Olling R. P. 1996, *AJ*, 112, 481  
Sackett P. 1997, *ApJ*, 483, 103  
Sackett, P. & Gould, A. 1993, *ApJ* 419, 648  
Sackett P., Rix H., Jarvis B.J., & Freeman K.C. 1994, *ApJ*, 436, 629